Exothermic reactions in cold-rolled Ni/Al reactive multilayer foils

X. Qiu and J. Graeter
Department of Mechanical Engineering, Louisiana State University, Baton Rouge, Louisiana 70803
L. Kecskes
United States Army Research Laboratory, Aberdeen Proving Ground, Maryland 21005
J. Wang[a)]
Department of Physics and Tsinghua–Foxcoon Nanotechnology Research Center, Tsinghua University, Beijing 100084, China; and Department of Mechanical Engineering, Louisiana State University, Baton Rouge, Louisiana 70803

(Received 3 April 2007; accepted 25 September 2007)

Exothermic reactions in cold-rolled Ni/Al reactive multilayer foils were investigated in this study. A two-stage reaction process was observed in the self-propagating reactions in the cold-rolled foils that were ignited by a point-source flame. Foils taken out of the flame after completing the first stage of the reaction process were compared to those allowed to complete both stages. Differences in the phase-evolution sequence from the two types of foils were studied by differential scanning calorimetry (DSC), using slow and controlled heating of the samples. Several exothermic peaks could be identified from the DSC thermograms for both types of foils. Using the DSC, both the as-cold-rolled and partially reacted foils were heated to each peak temperature to identify the reaction product associated with each peak. X-ray diffraction and scanning electron microscopy analyses showed that the first two peaks corresponded to the formation of Al_3Ni, while the third peak corresponded to the formation of AlNi.

I. INTRODUCTION

Over the last decade, exothermic formation reactions have been reported to self-propagate in a variety of reactive systems, such as Ni/Al, Ti/Al, or Nb/Si multilayered foils.[1–3] These materials consist of alternating layers of reactants with a large negative enthalpy of mixing. The self-propagating high-temperature synthesis (SHS) reaction in these multilayers is driven by a reduction in chemical-bond energy. The local reduction in chemical-bond energy produces a large quantity of heat that is conducted down the multilayers and facilitates further atomic mixing and compound formation. If atomic mixing and energy release occur sufficiently fast, compared to heat losses, then the reactions are self-sustaining. SHS reactions can be initiated in these multilayers at room temperature with a small thermal pulse. Such exothermic reactions in multilayers can be used as local heat sources to melt solders or brazes and thus join components in a variety of applications, such as making stainless steel–stainless steel, Al–Al, Ti–Ti, SiC–Ti, Si–Si, and bulk metallic glass (BMG)–BMG joints.[4–10]

Reactions in the Ni/Al multilayer system have been extensively investigated both theoretically and experimentally. Reactive multilayers are generally fabricated using physical vapor deposition (PVD) methods, such as magnetron sputtering or electron-beam evaporation. In PVD multilayers, Ma et al.[11] performed calorimetric measurements on Ni/Al multilayer films prepared by electron-beam evaporation. It was demonstrated that, under controlled annealing conditions, the formation of the single Al_3Ni product phase took place in two stages. The first stage is the nucleation, growth, and formation of a continuous layer, kinetically separated from the one-dimensional thickening growth stage, resulting in two separate calorimetric peaks.[11] Similar results were also obtained by Barmak et al. using sputtered Ni/Al multilayer films.[12] Ma et al.[11] attempted to investigate the processes preceding Al_3Ni formation and found that the Ni and Al composition profiles broadened upon annealing to a stage prior to Al_3Ni nucleation, indicating that interdiffusion had taken place. They interpreted that the interdiffused region was mainly composed of solid solutions. Edelstein et al. found that in Ni/Al multilayer films prepared by ion-beam deposition, the first phase to form can be AlNi, Al_3Ni, or Al_9Ni_2, depending on the overall stoichiometry and the modulation period of the multilayers.[13] Barmak and co-workers found that the B2 AlNi phase and an amorphous phase were formed during deposition of the multilayers made by magnetron sputtering,

[a)]Address all correspondence to this author.
e-mail: jpwang@tsinghua.edu.cn
DOI: 10.1557/JMR.2008.0043

which considerably reduced the driving force for subsequent reactions.[12] Depending on the periodicity of the multilayers, formation of Al_3Ni or Al_9Ni_2 followed by Al_3Ni was observed in their study. In the work of Blobaum et al.,[14] Al_9Ni_2 was the first phase to form in a series of Ni/Al multilayers except for a very small bilayer period (12.5 nm), where Al_3Ni was the first phase observed.

Alternatively, multilayer foils can also be made by cold-rolling methods.[15–18] In the cold-rolled Ni/Al multilayer foils, Battezzati,[17] Sieber,[15] and Qiu[16] all demonstrated that the first detectable phase to form was Al_3Ni. However, more recently, work done by Sauvage et al.[19] on cold-rolled Ni/Al multilayers revealed that a severe deformation process can induce metastable or nonequilibrium solid solutions with various compositions prior to the formation of any new product phase.

We have observed that SHS reactions of cold-rolled Ni/Al foils, ignited by a point-source flame, undergo a two-stage reaction process. To establish the nature and identity of the reaction product from the first stage, foils removed from the flame after completing the first stage of the reaction process were compared to those allowed to complete both stages. Further differences in the phase evolution in the two types of foils were studied by differential scanning calorimetry (DSC), using slow and controlled heating of the samples. Multiple exotherms could be identified for both types of foils. Using the DSC, both the as-cold-rolled and partially reacted foils were heated to each peak temperature to identify the reaction product associated with each exothermic peak. X-ray diffraction (XRD) and scanning electron microscopy (SEM) analyses showed that the first two peaks corresponded to the formation of Al_3Ni, while the third peak corresponded to the formation of AlNi.

II. EXPERIMENTAL PROCEDURES

Ni/Al multilayer foils were fabricated by a cold-rolling method using a laboratory rolling mill with a roller diameter of 65 mm. Figure 1 shows the schematic of the cold-rolling procedure. Thin sheets of pure elements of Ni and Al with initial thicknesses of 25.4 and 38.1 μm, respectively (McMaster-Carr Company, Los Angeles, CA; Ni minimum purity of 99.6 wt% and Al minimum purity of 99 wt%) were alternatively stacked together to obtain a 1:1 atomic ratio of Ni/Al [Figs. 1(a) and 1(b)]. The stacked sheets were then rolled to form a tube [Fig. 1(c)]. Two tubes were made at the same time with the same number of Ni/Al layers. Ni was the outer layer for one tube and Al was the outer layer for the other tube. These two tubes were flattened by a vise, put in a folded stainless steel sheet that had been previously hardened by repeated rolling, and cold-rolled a few times to reduce the thickness to half of their original thickness [Fig. 1(d)]. Afterward, they were taken out of the stainless steel sheet and stacked together to recover the original thickness. In this way, two same metal layers would not become layered side-by-side in the final multilayer foil. The stacked foils were then cold-rolled without changing the distance between the rollers. The thickness of the foil was reduced to half in one rolling pass. Subsequently, the resulting foils were cut into halves, stacked together, and the rolling procedure mentioned above was repeated for several times until a uniform multilayer foil was achieved [Figs. 1(e)–1(g)].

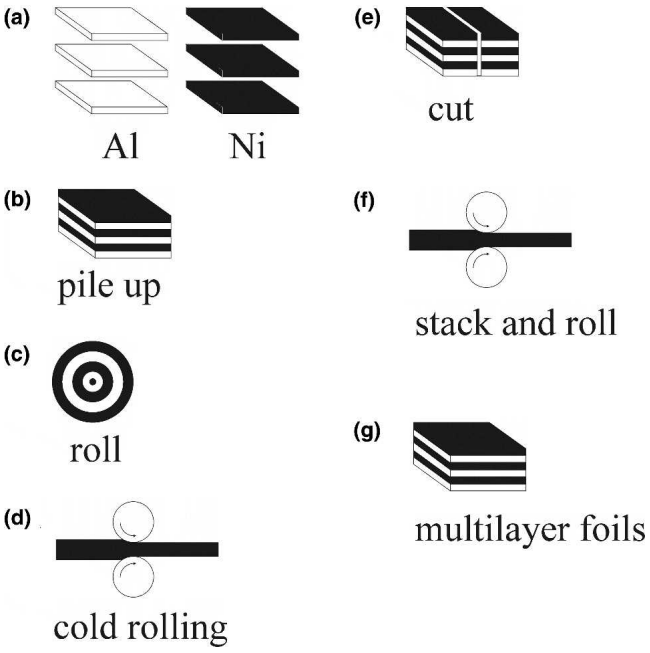

FIG. 1. Schematic of the cold-rolling procedure.

SHS reactions in the cold-rolled Ni/Al multilayer foils were initiated by heating one end of the foils in a flame with a temperature ≈500 °C in air for several seconds. The reaction velocities were measured under such conditions using a digital camcorder, with a temporal resolution of 0.03 s. The dimensions of the foils were 0.2 mm × 0.5 mm × 2.5 mm. To characterize the reaction products, the reacted Ni/Al foils were ground into powders for symmetric XRD examination using Cu K_α radiation. The unreacted, as-cold-rolled Ni/Al foils were also examined by XRD for comparison. Cross sections of as-cold-rolled and reacted foils were polished and then characterized by SEM using an S-3600N scanning electron microscope (Hitachi, Tokyo, Japan) equipped with energy-dispersive x-ray analysis (EDX) capability. The reacted foil was etched by electropolishing to reveal the grain boundaries, where the reacted foil was used as the anode and a graphite bar was used as the cathode. The electrolyte was a mixture of 80% acetic acid and 70% perchloric acid with a volume ratio of 9:1. The electropolishing process was conducted under 20 V at room temperature for 10 min.

The evolution of heat from the reaction process of the as-cold-rolled foil was measured using a PerkinElmer (Waltham, MA) DSC7 differential scanning calorimeter. In each DSC run, ≈10 mg of multilayer foil was heated from 50 to 725 °C at a rate of 40 °C/min in flowing N_2. Because the reaction was still not entirely completed at 725 °C, additional DSC runs were performed to 1000 °C to ensure that all reactants were consumed. A baseline was obtained by repeating the heating cycle, which was then subtracted from the heat-flow data obtained in the first run. By integrating the net heat flow with respect to time, the heat of reaction was obtained. Ni/Al multilayer foils made by magnetron sputtering (Reactive Nano-Technologies Inc., Hunt Valley, MD; total foil thickness, 40 μm, and bilayer thickness, 70 nm) were also examined by XRD and DSC for comparison. Note, because the PVD Ni/Al foils were made by magnetron sputtering, Ni layers contained ≈7 wt% V, an alloying element in the Ni sputter source. Therefore, it was expected that the presence of V would lower the total heat output from the PVD foil.

III. RESULTS AND DISCUSSION

A. Characterization of the SHS-reacted cold-rolled and PVD foils

The SHS reaction was initiated in the cold-rolled foil after one end of the foil was heated in a flame for several seconds. A two-stage reaction process was observed. In stage one, the reaction spread along the direction parallel to the surface of the foil at a relatively slow rate and the foil surface became darker. The darkening is most likely associated with the formation of surface oxides or nitrides of the reactant Al or Ni. In stage two, the reaction propagated at a much higher speed across the foil, releasing a much larger amount of heat and causing the foil to emit visible red light. Due to their much faster reaction propagation velocities, no such stepwise process could be observed for the PVD foils.

Figures 2 and 3 show the XRD traces from an unreacted as-cold-rolled multilayer and a PVD foil, both before and after the SHS reaction. For the unreacted foils, all the peaks in the XRD scan correspond to Ni and Al. The trace for the PVD foil contains only four Bragg reflection peaks, namely, for Al, (111) and (222), and for Ni, (111) and (222). The trace for the unreacted as-cold-rolled foil contains most of the Ni and Al crystal orientation reflections. In contrast, the traces for the reaction products from both the cold-rolled and the PVD foils are very similar, which were identified as the ordered B2 AlNi compound. Because the reacted cold-rolled foils and PVD foils were ground into powders for XRD examination, no texture could be observed in the reaction products.

Figures 4(a) and 4(b) show SEM images of the as-

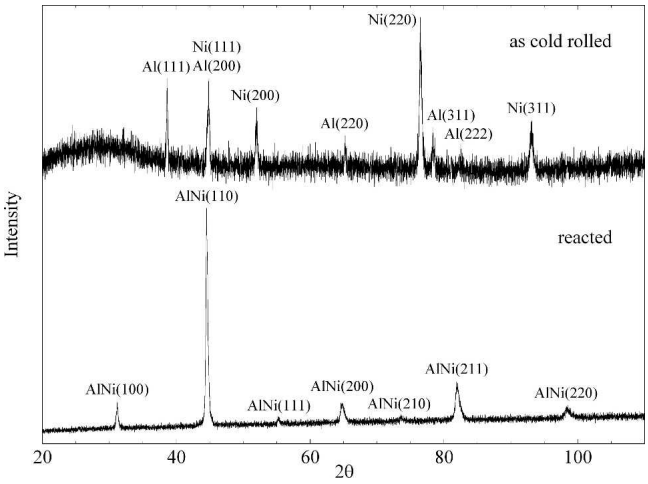

FIG. 2. XRD patterns of a cold-rolled multilayer foil and its SHS-reacted reaction product.

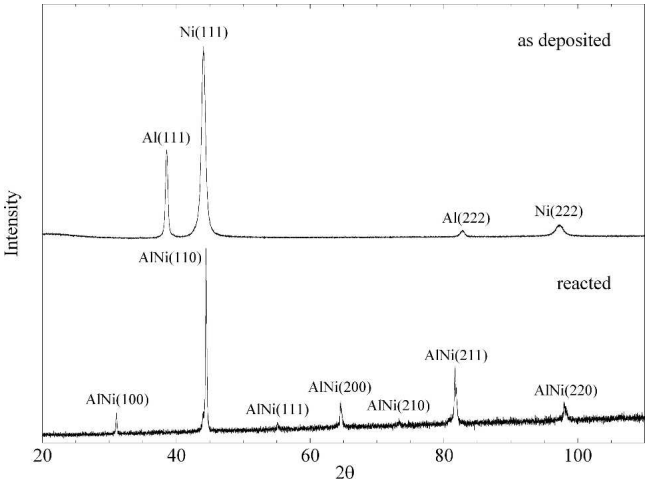

FIG. 3. XRD patterns of a PVD foil and its SHS-reacted reaction product.

cold-rolled Ni/Al foil and a foil that was reacted. Typically, in the as-cold-rolled Ni/Al multilayer foils, necked Ni particles are embedded in the Al matrix and aligned along the rolling direction [see Fig. 4(a)]. Most of the Ni particles possess a wavy surface. The average bilayer thickness of the as-cold-rolled foils is ≈10 μm, which is much thicker than those found in most PVD foils. In comparison, the PVD foils typically have bilayer thicknesses in the range of tens of nanometers.[2]

As shown in Fig. 4(b), two phases can be observed in the reacted cold-rolled foil: the primary reaction product, AlNi, and some Ni-rich phase. Although there is some backscattered electron contrast between the AlNi phase and the Ni-rich phase, the amount of the Ni-rich phase is very limited, and therefore it could not be identified with XRD [see Fig. 2]. Because the AlNi phase field is stable for a wide range of Ni contents (42–67 at.%), it is surmised that this contrast is most likely associated with a

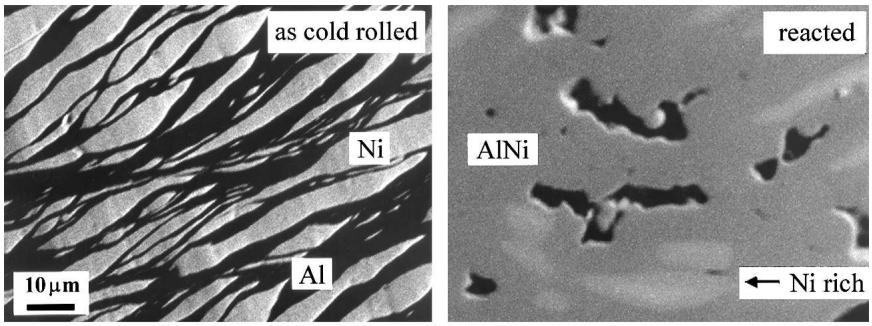

FIG. 4. SEM images of a cold-rolled multilayer foil and its SHS-reacted reaction product.

Ni-rich variant of AlNi. Some pores in the reacted foil are also observed, which arise from contraction during rapid cooling and density increase during the reaction. Figure 5 shows an SEM image of a reacted cold-rolled Ni/Al foil after electropolishing. The average AlNi grain size was estimated to be ≈15 μm. The lack of the Ni-rich phase on the sample surface might be due to a faster etching rate of the Ni-rich phase than that of AlNi during electropolishing.

The measured reaction velocities for the first reaction stage were ≈7 mm/s for five pieces of foils, which was much slower than the reaction speed in the Ni/Al multilayer foils made by PVD methods that have reaction velocities ranging between 1 and 30 m/s.[20,21] The lower speed in the cold-rolled foils was due to the much larger Ni/Al bilayer thickness. As the bilayer thickness becomes larger, the atomic diffusion distances are longer, and, therefore, atoms mix more slowly. As such, heat is released at a lower rate, and the reactions travel more slowly through the foil. In addition, the alternating Ni/Al layers in the cold-rolled foil were not uniform, thus making it difficult to ignite the foil and reducing the speed of the self-propagating reaction. Despite such shortcomings in the cold-rolled multilayer foils, this method has its own advantages, such as ease of fabrication, low cost, and less time-consuming nature. Meanwhile, the reduction in reaction velocity also made the cold-rolled foil an ideal system to study the details of the formation reactions in multilayer foils.

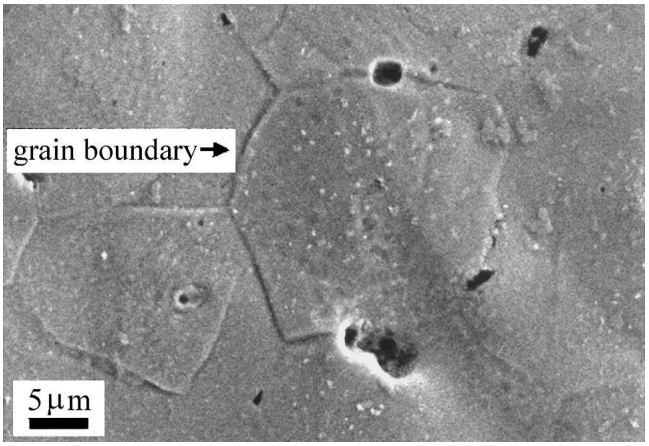

FIG. 5. SEM image of a cold-rolled Ni/Al foil after complete SHS reaction and electropolishing.

B. Characterization of the DSC-reacted cold-rolled and PVD foils

As shown in Fig. 6, the DSC curve of the as-cold-rolled Ni/Al multilayer foil reveals the convolution of three peaks. The very large broad peak, centered on position C, contains a superimposed peak appearing as a shoulder (position A), and a sharp peak (position B). For comparison, a DSC curve for a PVD foil with a bilayer thickness of 70 nm is also included in the figure. There are three well-separated peaks in the latter curve; the lowest temperature peak is actually a superposition of two peaks.

The peak shapes of the two types of DSC curves are different. First, the peak temperatures for the cold-rolled foil are much higher than those for the PVD foil. This is due to the much larger bilayer thickness (around 10 μm for the cold-rolled foils versus tens of nanometers for the PVD foils) and the nonuniform structure of the cold-rolled foils. Second, although the peak positions identified by the letters in the cold-rolled foil are well separated along the temperature axis, they are on top of a very large broad "feature" that seems to dominate the entire thermal process. Third, the peak profiles in the two foil types are not the same; such differences are indicative of

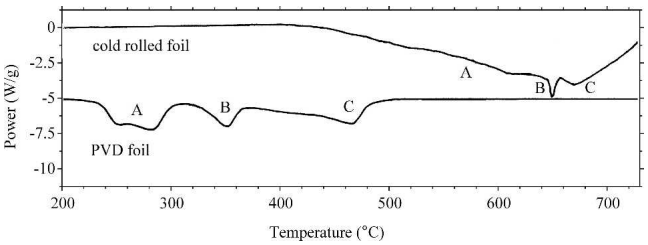

FIG. 6. DSC curves for an as-cold-rolled Ni/Al multilayer foil and an as-deposited PVD Ni/Al multilayer foil.

different underlying reaction mechanisms. Last, notable differences in the relative peak amplitudes are reflective of the extent of contributions (both heat output and phase formation) to the overall reaction sequence.

To identify the evolution of reaction products from the different reaction stages for the cold-rolled Ni/Al multilayer foils, some as-cold-rolled foils were heated to 350 °C (slightly below the onset temperature of the shoulder peak A in the DSC curve), 530 °C (the midpoint temperature of peak A), 640 °C (the midpoint temperature of peak B), and 725 °C (the maximum temperature for the DSC scans) using the same heating rate as in the previous DSC runs. Figure 7 shows the XRD pattern and SEM image for the cold-rolled foil heated to 350 °C. They are similar to those for the as-cold-rolled foils. Only Ni and Al can be identified in the annealed foil.

For the as-cold-rolled foil heated to 530 and 640 °C [Figs. 8(a) and 8(b)], Al_3Ni peaks appear among the Ni and Al peaks, suggesting that Al_3Ni was generated at these temperatures. For the foil annealed to 530 °C, Al_3Ni layers can be observed at isolated sites along the Ni/Al interface. The inset in Fig. 8(a), suggests that position A in the DSC curve is associated with the growth of Al_3Ni at isolated nucleation sites. In the foil annealed to 640 °C, the Al_3Ni layers are continuous, fully covering the Ni particles. Also, growth in thickness along the direction normal to the surface toward neighboring Ni particles can be observed [see Fig. 8(b)]. This suggests that peak B in the DSC curve is related to the growth of Al_3Ni in the direction normal to the Ni/Al interface. Therefore, both DSC peak positions A and B in the curve of the cold-rolled Ni/Al multilayer foils are associated with the exothermic formation of Al_3Ni. This is in agreement with earlier qualitative interpretations of the two exothermic DSC peaks that were observed for the formation of a single phase.[11,22] However, in Coffey's and Ma's models, it was assumed that the generation of Al_3Ni occurred

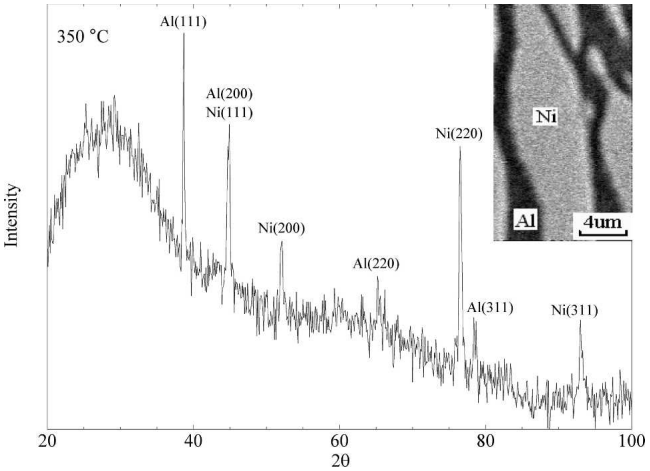

FIG. 7. XRD pattern and SEM image for the as-cold-rolled Ni/Al multilayer foils heated to 350 °C in the DSC.

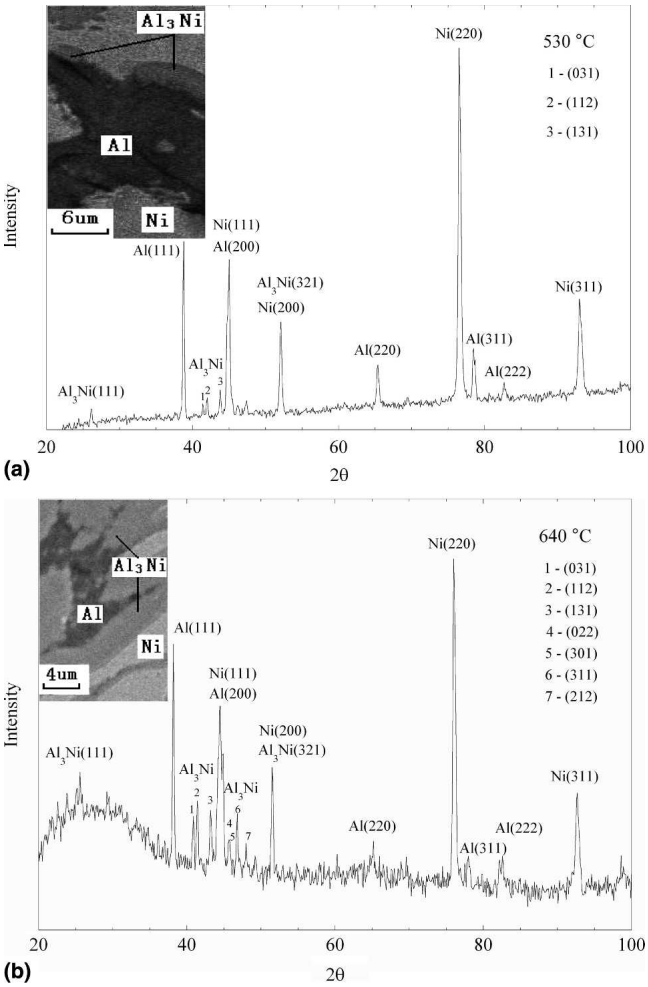

FIG. 8. (a) XRD pattern and SEM image for the as-cold-rolled Ni/Al multilayer foils heated to 530 °C in the DSC. (b) XRD pattern and SEM images for the as-cold-rolled Ni/Al multilayer foils heated to 640 °C in the DSC.

as a two-stage process in reactive foils where the reactant interspacing was significantly reduced. The first step was the lateral growth of the Al_3Ni phase from isolated nucleation sites and the subsequent coalescence into a continuous layer. The second step was the growth of such Al_3Ni layers in the direction normal to the interface until all Al was consumed.

Our XRD and SEM results do not precisely support Coffey's model for the two-stage formation process of Al_3Ni. Specifically, as shown in Fig. 6, the size and shape of peaks A and B do not match Coffey's model. It is likely that such an extrapolation to a greater separation of the reactants, manifested in the cold-rolled foils, cannot be made. Instead, reactions in the cold-rolled foils might be governed by another mechanism.

In the DSC curve for the cold-rolled foils, the first peak is broad and the second peak is sharper and very small. This is partially due to the nonuniform interfacial area in the cold-rolled foils. The triangular shape of peak A is consistent with a diffusion-controlled process. There

is a definite change in the growth mode of the Al_3Ni layer as indicated by the appearance of peak B. Because for the as-cold-rolled foils heated to 725 °C (Fig. 9), three to four phases can be identified: the intermediate reaction product Al_3Ni, a Ni-rich phase, unreacted Ni, and the final reaction product, AlNi. As such, peak C in the DSC curve must be associated with the formation of AlNi. It is interesting that, at 725 °C, a considerable amount of Ni is still present in the foil. Note, however, that there might be some other intermetallic phases, such as Al_3Ni_2, during the transition from Al_3Ni to AlNi, which require further investigation in the future.

By integrating the net heat flow with respect to time of the DSC data up to 1000 °C (not shown), heats of reaction for the cold-rolled and the PVD foils were calculated to be −57.5 and −57.9 kJ/mol, respectively. The calculated values carry a measurement/calculation error of about ±0.5 kJ/mol and are slightly smaller than the formation enthalpy of AlNi (−59 kJ/mol).[23] The slightly smaller heats of reaction might be due to several factors, such as prior intermixing that occurs during the multilayer fabrication process. For the PVD foils, the presence of V would also lower the total heat output. For the cold-rolled foil, the reaction products are not entirely AlNi but contain a Ni-rich AlNi phase; this would likewise cause a lower measured heat of reaction compared to the literature value.

After the first-stage reaction was completed in self-propagating reactions, some cold-rolled foils were taken out of the flame to terminate the reaction in the middle of the foils. The XRD trace for the partially reacted foil (not shown) was similar to the trace of the as-cold-rolled foil, containing only Ni and Al peaks. The DSC curve for the partially reacted foil is shown in Fig. 10. Note that there are also three exothermic peaks in this DSC scan. Although XRD was not sensitive to detect subtle differences, unlike the DSC trace shown in Fig. 6, the thermal rise to peak A is not as steep, and peak B is clearly preceded by a sharp endotherm.

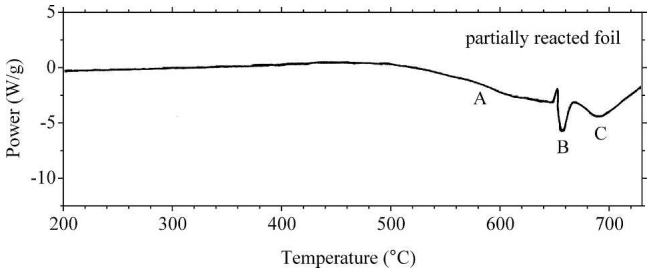

FIG. 10. DSC curve for the partially reacted cold-rolled Ni/Al multilayer foil.

To identify the reaction products for the different reaction stages, some of the partially reacted foils were heated to 350 °C (below the onset temperature of peak A), 550 °C (the midpoint temperature of peak A), 660 °C (the midpoint temperature of peak B), and 725 °C (the maximum temperature for the DSC scans) using the same heating rate as in the previous DSC runs. Figure 11 shows the XRD patterns and a SEM image for the partially reacted foil heated to 350 °C. The as-cold-rolled foil annealed to 350 °C only contained Ni and Al (Fig. 7). In contrast, in the partially reacted foil that was annealed to 350 °C, Al_3Ni layers (the Ni/Al atomic ratio obtained by EDX is approximately 1:3) can be observed at isolated sites at the Ni/Al interface. Obviously, due to the small amount of Al_3Ni formed, it could not be identified from the XRD scan. This difference between the as-cold-rolled and partially reacted cold-rolled foils confirms that the first reaction stage observed in the SHS reaction is associated with growth of Al_3Ni at isolated nucleation sites near the Ni/Al interface.

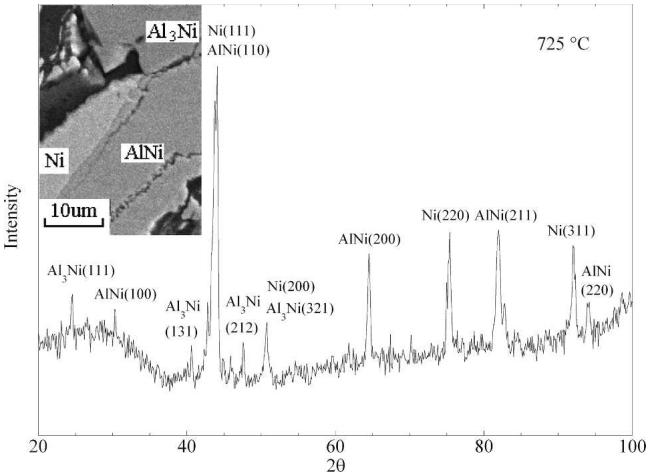

FIG. 9. XRD pattern and SEM image for the as-cold-rolled Ni/Al multilayer foils heated to 725 °C in the DSC.

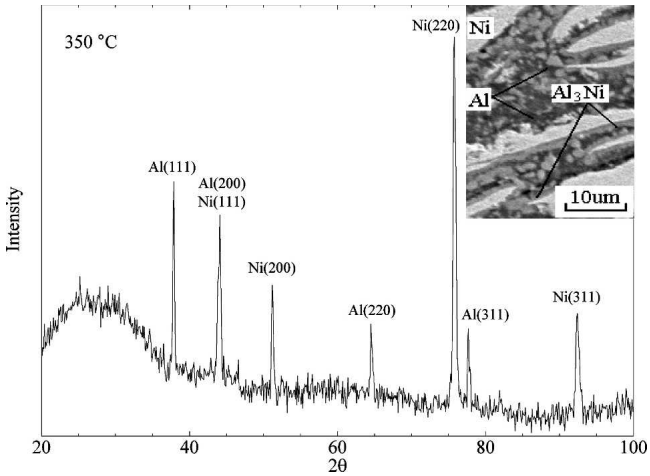

FIG. 11. XRD pattern and SEM image for the partially reacted cold-rolled Ni/Al multilayer foils heated to 350 °C in the DSC.

For the partially reacted foils heated to 550 and 660 °C, the XRD traces and SEM images provide similar results to the cold-rolled foils that were heated to 530 and 640 °C. For the partially reacted foil heated to 550 °C, Al_3Ni layers appear at isolated sites along the Ni/Al interface [Fig. 12(a)], and for the partially reacted foil heated to 660 °C, the Al_3Ni layers become continuous, cover the Ni particles completely, and grow in thickness toward the neighboring Ni particles [Fig. 12(b)]. Thus, the first two peaks (A and B in Fig. 10) in the DSC curve of the partially reacted Ni/Al multilayer foil could also be identified as the exothermic formation of Al_3Ni. Similar to the as-cold-rolled foils that were annealed to 725 °C, for the partially reacted foils heated to 725 °C (Fig. 13), there are also three to four phases in the foil: Al_3Ni, a Ni-rich phase, unreacted Ni, and the primary reaction product, AlNi. Thus, peak C in the DSC scan for the partially reacted foils is associated with the formation of the final product, AlNi.

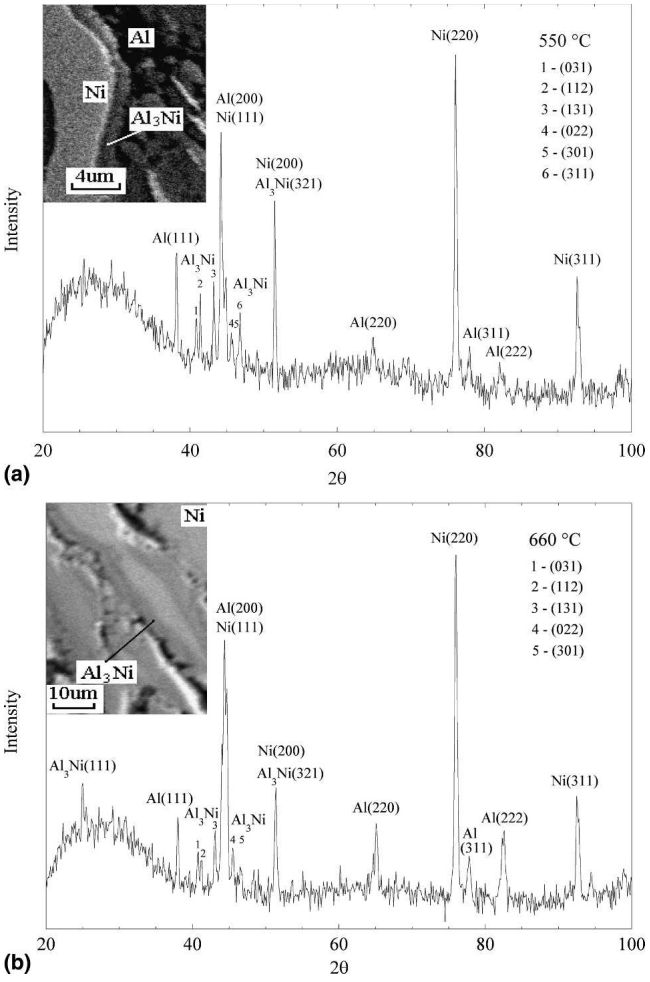

FIG. 12. (a) XRD pattern and SEM image for the partially reacted cold-rolled Ni/Al multilayer foils heated to 550 °C in the DSC. (b) XRD pattern and SEM images for the partially reacted cold-rolled Ni/Al multilayer foils heated to 660 °C in the DSC.

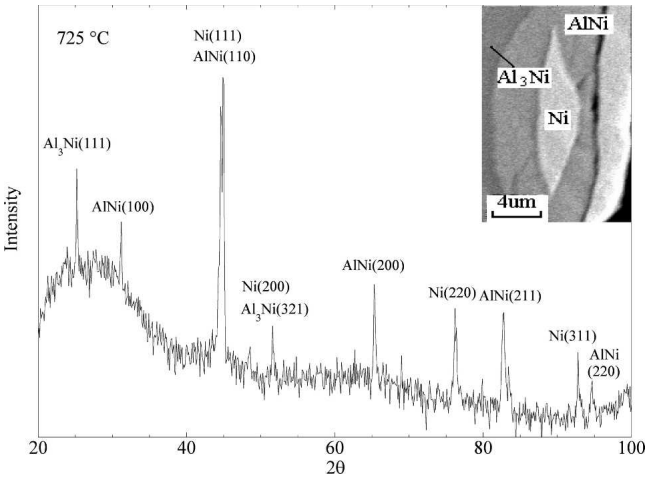

FIG. 13. XRD pattern and SEM image for the partially reacted cold-rolled Ni/Al multilayer foils heated to 725 °C in the DSC.

While there are strong similarities, there are also some differences between the DSC curves of the as-cold-rolled foil and the partially reacted cold-rolled foil. Peak A of the partially reacted foils (onset at ≈500 °C) is much smaller than that of the as-cold-rolled foils (onset at ≈430 °C), which suggests that the first stage of reaction has already occurred in the partially reacted foils. The diminished energy release in the DSC experiment is self evident, as a partial conversion of the reactants to product has already occurred. The transition from a diffusion-controlled to a precipitation-type mechanism is also more pronounced in the partially reacted foil with the appearance of the endothermic peak that precedes peak B. The endotherm onset appears at ≈640 °C, corresponding to the melting of Al–Ni eutectic. Also, the three peak temperatures for the partially reacted foils are higher compared with the as-cold-rolled foils, indicating that more energy input from DSC is needed to complete the same phase-formation process. Again, these higher peak temperatures are due to the occurrence of the first stage of the SHS reaction prior to the DSC anneal experiments in the partially reacted foils.

From data presented in the DSC curves, SEM observations, and XRD scans from both as-cold-rolled and partially reacted cold-rolled Ni/Al multilayer foils at various formation stages, some of the SHS reaction process for cold-rolled Ni/Al multilayer foils could be identified. Based on differences between the as-cold-rolled and partially reacted foils, it may be concluded that the first reaction stage, with a slow reaction velocity, corresponds to the nucleation and growth of Al_3Ni phase at isolated sites. This stage was associated with peak A in the DSC curve.

Because reaction velocities exhibited in the SHS reaction in the second stage are extreme, the DSC results cannot be used to elucidate the sequential formation of

AlNi. However, the initial Al_3Ni phase must follow some sequential conversion to the final AlNi phase. That process is likely much faster than that observed in the DSC measurements and will not follow the observed diffusional growth of the Al_3Ni layer. Moreover, the balance between heat generation and loss is expected to be so different that a precipitation reaction more likely occurs in the SHS process.

In the DSC, under slow, controlled annealing conditions, the Al_3Ni nuclei grow in the direction parallel to the Ni/Al interface and subsequently coalescence into a continuous layer. Growth of the Al_3Ni layers in the direction normal to the Ni/Al interface continues until all Al is consumed. However, with increased heat generation in the DSC-heated foils, the mechanism switches from a diffusion-controlled to a precipitation-controlled process. This stage was related to peak B in the DSC curve. The change in kinetics causes the Al_3Ni to react with the remaining Ni-rich phase to form the final reaction product, AlNi, corresponding to peak C and beyond in the DSC scan.

IV. CONCLUSIONS

Ni/Al multilayer foils were fabricated by a cold-rolling method. After ignition, a two-stage SHS reaction process was observed. In stage one, the reaction spread along the lateral direction to the surface of the foil at a relatively slow rate and the foil surface became darker. In stage two, the reaction occurred at a much higher speed and released a large amount of heat, emitting visible red light. The final reaction product was AlNi.

Based on a comparison of foils that were partially reacted up to the first stage to those that reacted completely, we may conclude that the first SHS reaction stage, with a slow reaction velocity, is associated with the nucleation and limited lateral growth of Al_3Ni phase at isolated sites. Further heating under controlled conditions causes these nuclei to coalescence into a continuous layer. Therefore, the second SHS reaction stage, with a fast reaction velocity, must be the growth of the Al_3Ni layers in the direction normal to the Ni/Al interface until all Al is consumed, with a subsequent reaction of Al_3Ni with the remaining Ni-rich phase to form and convert into the final reaction product, AlNi.

DSC experiments showed qualitative agreement with prior models that describe a sequential formation (nucleation and lateral growth) of a single phase in multilayer foils. However, the observed shapes of the exothermic peaks in the DSC profiles from the cold-rolled foils do not agree with the peak shapes used to model the reaction sequence. It is likely that the greater separation of the reactants and the nonuniformity of the foil's microstructure have contributed to obscuring the shapes of the exothermic peak doublet. The nonuniform morphology of the cold-rolled foils also alters the nucleation kinetics, wherein a lesser surface area may present itself to available nucleation sites. As such, the initial peak would become broader, thereby reducing the heat that would evolve under the second peak.

ACKNOWLEDGMENT

This work was supported by the National Science Foundation (Award DMI-0556100).

REFERENCES

1. E. Ma, C.V. Thompson, L.A. Clevenger, and K.N. Tu: Self-propagating explosive reactions in Al/Ni multilayer thin films. *Appl. Phys. Lett.* **57,** 1262 (1990).
2. T.P. Weihs: *Handbook of Thin Film Process Technology* (Institute of Physics, Bristol, UK, 1998), pp. F7:1, F7:13.
3. M.E. Reiss, C.M. Esber, D. Van Heerden, A.J. Gavens, M.E. Williams, and T.P. Weihs: Self-propagating formation reactions in Nb/Si multilayers. *Mater. Sci. Eng., A* **261,** 217 (1999).
4. J. Wang, E. Besnoin, A. Duckham, S.J. Spey, M.E. Reiss, O.M. Knio, and T.P. Weihs: Joining of stainless-steel specimens with nanostructured Al/Ni foils. *J. Appl. Phys.* **95,** 248 (2004).
5. J. Wang, E. Besnoin, O.M. Knio, and T.P. Weihs: Effects of physical properties of components on reactive nanolayer joining. *J. Appl. Phys.* **97,** 4307 (2005).
6. A. Duckham, S.J. Spey, J. Wang, M.E. Reiss, and T.P. Weihs: Reactive nanostructured foil used as a heat source for joining titanium. *J. Appl. Phys.* **96,** 2336 (2004).
7. J. Wang, E. Besnoin, A. Duckham, S.J. Spey, M. Reiss, O.M. Knio, M. Powers, M. Whitener, and T.P. Weihs: Room-temperature soldering with nanostructured foils. *Appl. Phys. Lett.* **83,** 3987 (2003).
8. A.J. Swiston, Jr., T.C. Hufnagel, and T.P. Weihs: Joining bulk metallic glass using reactive multilayer foils. *Scripta Mater.* **48,** 1575 (2003).
9. J. Wang, E. Besnoin, O.M. Knio, and T.P. Weihs: Investigating the effect of applied pressure on reactive multilayer foil joining. *Acta Mater.* **52,** 5265 (2004).
10. X. Qiu and J. Wang: Reactive multilayer foils for silicon wafer bonding, in *Advanced Electronic Packaging*, edited by V.P. Atluri, S. Sharan, C-P. Wong, and D. Frear (Mater. Res. Soc. Symp. Proc. **968,** Warrendale, PA, 2007), p. 968-V02-06.
11. E. Ma, C.V. Thompson, and L.A. Clevenger: Nucleation and growth during reactions in multilayer Al/Ni films: The early stage of Al_3Ni formation. *J. Appl. Phys.* **69,** 2211 (1991).
12. K. Barmak, C. Michaelsen, and G. Lucadamo: Reactive phase formation in sputter-deposited Ni/Al multilayer thin films. *J. Mater. Res.* **12,** 133 (1997).
13. A.S. Edelstein, R.K. Everett, G.Y. Richardson, S.B. Qadri, E.I. Altman, J.C. Foley, and J.H. Perepezko: Intermetallic phase formation during annealing of Al/Ni multilayers. *J. Appl. Phys.* **76,** 7850 (1994).
14. K.J. Blobaum, D. Van Heerden, A.J. Gavens, and T.P. Weihs: Al/Ni formation reactions: Characterization of the metastable Al_9Ni_2 phase and analysis of its formation. *Acta Mater.* **51,** 3871 (2003).
15. H. Sieber, J.S. Park, J. Weissmüller, and H. Perepezko: Structural evolution and phase formation in cold-rolled aluminum–nickel multilayers. *Acta Mater.* **49,** 1139 (2001).

16. X. Qiu and J. Wang: Experimental evidence of two-stage formation of Al_3Ni in reactive Ni/Al multilayer foils. *Scripta Mater.* **56,** 1055 (2007).
17. L. Battezzati, P. Pappalepore, F. Purbiano, and I. Gallino: Solid state reactions in Al/Ni alternate foils induced by cold rolling and annealing. *Acta Mater.* **47,** 1901 (1999).
18. T.P. Weihs and M. Reiss: Method of making reactive multilayer foil and resulting product. U.S. Patent No. 6 534 194 (May 18, 2003).
19. X. Sauvage, G.P. Dinda, and G. Wilde: Non-equilibrium intermixing and phase transformation in severely deformed Al/Ni multilayers. *Scripta Mater.* **56,** 181 (2007).
20. A.B. Mann, A.J. Gavens, M.E. Reiss, D. Van Heerden, G. Bao, and T.P. Weihs: Modeling and characterizing the propagation velocity of exothermic reactions in multilayer foils. *J. Appl. Phys.* **82,** 1178 (1997).
21. A.J. Gavens, D. Van Heerden, A.B. Mann, M.E. Reiss, and T.P. Weihs: Effect of intermixing on self-propagating exothermic reactions in Al/Ni nanolaminate foils. *J. Appl. Phys.* **87,** 1255 (2000).
22. K.R. Coffey, L.A. Clevenger, K. Barmak, D.A. Rudman, and C.V. Thompson: Experimental evidence for nucleation during thin-film reactions. *Appl. Phys. Lett.* **55,** 852 (1989).
23. R. Pretorius, A.M. Vredenberg, F.W. Saris, and R. de Reus: Prediction of phase formation sequence and phase stability in binary metal–aluminum thin-film systems using the effective heat of formation rule. *J. Appl. Phys.* **70,** 3636 (1991).